

## A 222 Energy Bins Response Matrix for a <sup>6</sup>LiI Scintillator BSS system

Marco A. S. Lacerda<sup>1</sup>, Hector Rene Vega-Carrillo<sup>2</sup>, Roberto Méndez-Villafañe<sup>3</sup>  
Alfredo Lorente-Fillol<sup>4</sup>, Sviatoslav Ibañez-Fernandez<sup>4</sup>, Eduardo Gallego-Díaz<sup>4</sup>

<sup>1</sup>Laboratório de Calibração de Dosímetros, Centro de Desenvolvimento da Tecnologia Nuclear, CDTN/CNEN, Av. Presidente Antonio Carlos, 6627, 31270-901, Belo Horizonte, Brazil, [masl@cdtn.br](mailto:masl@cdtn.br)

<sup>2</sup>Unidad Académica de Estudios Nucleares, Universidad Autónoma de Zacatecas, UAZ, Apdo. Postal 336, 98000, Zacatecas, Zac, Mexico

<sup>3</sup>Laboratorio de Patrones Neutrónicos, Centro de Investigaciones Energéticas, Medioambientales y Tecnológicas, CIEMAT, Av. Complutense, 22, 28040, Madrid, España

<sup>4</sup>Departamento de Ingeniería Nuclear  
Universidad Politécnica de Madrid, UPM, 28006, Madrid, España,

### Abstract

A new response matrix was calculated for a Bonner Sphere Spectrometer (BSS) with a <sup>6</sup>LiI(Eu) scintillator. We utilized the Monte Carlo N-Particle radiation transport code MCNPX, version 2.7.0, with ENDF/B-VII.0 nuclear data library to calculate the responses for 6 spheres and the bare detector, for energies varying from 9.441E(-10) MeV to 105.9 MeV, with 20 equal-log(E)-width bins per energy decade, totalizing 222 energy groups. A BSS, like the modeled in this work, was utilized to measure the neutron spectrum generated by the <sup>241</sup>AmBe source of the Universidad Politécnica de Madrid (UPM). From the count rates obtained with this BSS system we unfolded neutron spectrum utilizing the BUNKIUT code for 31 energy bins (UTA4 response matrix) and the MAXED code with the new calculated response functions. We compared spectra obtained with these BSS system / unfold codes with that obtained from measurements performed with a BSS system constituted of 12 spheres with a spherical <sup>3</sup>He SP9 counter (Centronic Ltd., UK) and MAXED code with the system-specific response functions (BSS-CIEMAT). A relatively good agreement was observed between our response matrix and that calculated by other authors. In general,

---

we observed an improvement in the agreement as the energy increases. However, higher discrepancies were observed for energies close to 1E(-8) MeV and, mainly, for energies above 20 MeV. These discrepancies were mainly attributed to the differences in cross-section libraries employed. The ambient dose equivalent ( $H^*(10)$ ) calculated with the  ${}^6\text{LiI-MAXED}$  showed a good agreement with values measured with the neutron area monitor Berthold LB 6411 and within 12% the value obtained with another BSS system (BSS-CIEMAT). The response matrix calculated in this work can be utilized together with the MAXED code to generate neutron spectra with a good energy resolution up to 20 MeV. Some additional tests are being done to validate this response matrix and improve the results for energies higher than 20 MeV.

**Keywords:** Monte Carlo, Neutron Spectrometry, Bonner sphere neutron spectrometer.

## 1.- INTRODUCTION

Neutron spectrometry is important for complete characterization of the radiation field in workplaces. From the neutron fluence spectrum, it is possible to determine the radiation protection quantities (absorbed dose in the body,  $D_T$ , and effective dose,  $E$ ) or operational quantities (dose equivalent personal  $H_p(d)$  and ambient dose equivalent  $H^*(10)$ ). Bonner multisphere spectrometry systems, more commonly known as Bonner Spectrometers Systems (BSS), are normally used for neutron spectrometry studies. BSS have the advantage of an almost isotropic response, covering a wide energy range from thermal to GeV [Bramblett *et al.*, 1960; Awschalow and Sanna 1985; Thomas and Alevra 2002; McDonald *et al.*, 2002].

BSS consist of a thermal neutron detector surrounded by a set of moderating polyethylene spheres of varying thickness. There is a response function for each detector/moderator, defined as the reading per unit fluence, as function of neutron energy. The response function is normally calculated using Monte Carlo (MC) codes and validated with measurements performed in standardized monoenergetic neutron fields [McDonald *et al.*, 2002; Mazrou *et al.*, 2010].

From the response functions, a response matrix ( $R$ ) with “ $m \times n$ ” values are created, where “ $m$ ” represents the matrix rows or the number of detector/moderating spheres and “ $n$ ” stands for the total number of energy bins considered. The Response matrix ( $R$ ) and BSS readings ( $M$ ), assumed contained in a vector of “ $n$ ” elements, are utilized to obtain the spectral information,  $\Phi$ , also assumed contained in a vector with “ $n$ ” elements. Then, a set of “ $m$ ” linear equations can be written as showed in Equation 1.

$$M = R \cdot \Phi \quad (1)$$

Neutron spectrum is derived by applying an inverse process, called unfolding procedure, that is a typical few-channel unfolding, since the number of individual measurements, “m”, is significantly smaller than the number of energy bins, “n”. There are some unfolding procedures utilized to provide a mathematical solution with an acceptable physical meaning for this under-determined problem. Linear and non-linear least-squares adjustments, the Bayesian theory, the principle of maximum entropy, Monte Carlo and approaches based on Artificial intelligence technology are the methods used for unfolding [Matzke 2002]. Many computerized BSS unfolding codes have been developed using the methods previously described, such as BON94, BUNKI / BUNKIUT, MAXED, FRUIT, BUMS, NSDUAZ and NSDann [Lowry *et al.*, 1984; Sweezy *et al.*, 2002; Reginatto *et al.*, 2002; Bedogni *et al.*, 2007; Sannikov 1994; Vega-Carrillo *et al.*, 2012; Martinez-Blanco *et al.*, 2009].

The accuracy of the spectral neutron fluence derived by any unfolding procedure using experimental readings of the BSS is limited by the accuracy of the appropriate response matrix. There are some published response functions available for BSS with <sup>6</sup>LiI detectors [Sanna 1973; Hertel and Davidson 1985; Mares and Schraube 1994; Vega-Carrillo *et al.*, 2008; Mazrou *et al.*, 2010], <sup>3</sup>He proportional counters [Mares *et al.*, 1991; Aroua *et al.*, 1992; Wiegel and Alevra 2002] and passive detectors [Bedogni *et al.*, 2008; Garny *et al.*, 2009; Vega-Carrillo *et al.*, 1999].

In this paper we utilized the Monte Carlo N-Particle radiation transport code MCNPX [Pelowitz 2011] to calculate the response functions of a Bonner Sphere Spectrometer (BSS) with a <sup>6</sup>LiI(Eu) scintillator. Then, a BSS, like the modeled in this work, was utilized to measure the total neutron spectrum generated by the <sup>241</sup>AmBe source of the Universidad Politécnica de Madrid (UPM). This spectrum was compared with that obtained with a BSS system with a <sup>3</sup>He proportional counter.

## 2.- MATERIALS AND METHODS

We utilized the Monte Carlo N-Particle radiation transport code MCNPX, version 2.7.0, with ENDF/B-VII.0 nuclear data library, to calculate the response functions of a Bonner Sphere Spectrometer (BSS) with a  $^6\text{Li}(\text{Eu})$  scintillator. We designed a realistic model of the cylindrical detector (0.4 cm x 0.4  $\varnothing$  cm) with its metallic cask, the light pipes and the polyethylene spheres. MC calculations were performed for the following sphere diameters, in inches: BALL 2 (2"), BALL 3 (3"), BALL 5 (5"), BALL 8 (8"), BALL 10 (10") and BALL 12 (12"). We also performed simulations with the bare detector, without a polyethylene sphere, BALL 0. Responses were calculated for all spheres and the bare detector for energies varying from 9.441E(-10) MeV to 105.9 MeV, with 20 equal-log(E)-width bins per energy decade, totalizing 222 energy groups. The number total of input files were  $7 \times 222 = 1554$ . Two Python programs were developed to aid rapid creation of input files for each sphere / energy bin and rapid extraction of the responses from output files.

Atomic composition and physical data were taken from Seltzer and Berger [1982]. We used  $S(\alpha,\beta)$  cross section tables for polyethylene (density = 0.95 g.cm<sup>-3</sup>) to take into account the chemical binding and crystalline effects on thermal neutron scattering at room temperatures [Pelowitz 2011]. For the scintillator crystal we adopted a density of 3.494 g.cm<sup>-3</sup> and the following mass fractions: 4.36E(-2), 1.8E(-1) and 9.546E(-1) for  $^6\text{Li}$ ,  $^7\text{Li}$  and  $^{127}\text{I}$ , respectively.

To ensure a uniform irradiation of the spheres, we assumed monoenergetic neutron sources like disks with the same diameters as the spheres. These disks were centered on and perpendicular to the axis of the detector. The environment between the source and the BSS system was treated as void. The response was defined as the number of  $^6\text{Li}(n, t)^4\text{He}$  reactions occurring within the scintillator, per each neutron incident neutron fluence

normalized to one starting particle. We utilized the Equation 2, in MCNPX, to obtain the response, R.

$$R = \Phi \cdot a_S \cdot n_{6Li} \cdot V_{det} \cdot \sigma(n, t) \quad (2)$$

Where,

$\Phi$  : particle fluence, in  $\text{cm}^{-2}$ , given by the tally 4, in MCNPX output;

$a_S$  : area of the neutron source, in  $\text{cm}^2$ ;

$n_{6Li}$  : number density, in  $(1\text{E}24 \cdot \text{cm}^{-3})$ ;

$V_{det}$  : sensitive detector volume, in  $\text{cm}^3$ ;

$\sigma(n, t)$  :  ${}^6\text{Li}(n, t){}^4\text{He}$  cross section, in barn. Reaction number MT=105 in MCNPX input.

The MCNPX was implemented to run under UNIX operating system on the EULER supercomputer, a high performance cluster (HPC) of CIEMAT, composed of 256 blades, 2x Intel Xeon 5450 Quad Core 3.0 GHz processors (2048 cores total). Between 8 and 16 processors were used to parallel processing/simulation of the inputs. The number of histories necessary to obtain uncertainties less than 3%, varied for each sphere / energy bin, from 1E6 to 3E8. The only variance reduction technique we utilized consisted of subdividing the spheres in a series of concentric shells, weighting the cells with different neutron importance. The closer the neutrons approach the counter volume, the higher is the importance.

A BSS system manufactured by the Ludlum Measurements, like the modeled in this work, was utilized to measure the neutron spectrum generated by the  ${}^{241}\text{AmBe}$  source of the Universidad Politécnica de Madrid (UPM). This source has an activity of  $111 \pm 10\%$  GBq and a nominal strength of  $6.64 \cdot 10^6 \text{ s}^{-1}$  on February 5, 1969.

Measurements were performed at 115 cm from the source, on the calibration bench, as showed in the Figure 1. From the count rates obtained with this BSS system (BSS-<sup>6</sup>LiI), we unfolded the total neutron spectrum ( $\Phi_{tot}$ ). Data were unfolded utilizing: (a) the BUNKIUT code [Lowry *et al.*, 1984] with the SPUNIT algorithm and UTA4 response matrix (31 energy bins) and; (b) MAXED computer code, from the UMG 3.3 package [Reginatto *et al.* 2004], with the new calculated response functions. We also compared spectra obtained with these BSS system / unfold codes with those obtained from measurements performed with a BSS system constituted of 12 spheres with a spherical <sup>3</sup>He SP9 counter (Centronic Ltd., UK). For this BSS system (BSS-<sup>3</sup>He), MAXED computer code from the UMG 3.3 package was also utilized with the system-specific response functions (CIEMAT-BSS), determined in the Physikalisch-Technische Bundesanstalt (PTB) (Braunschweig, Germany).

The initial guess spectrum utilized in all cases was that obtained with Monte Carlo calculations, from a previous model of the irradiation facility [Vega-Carrillo *et al.* 2012]. The neutron energy spectra were folded with fluence-to-ambient dose equivalent conversion coefficients, in pSv.cm<sup>2</sup>, from the ICRP 74 [ICRP 1996].

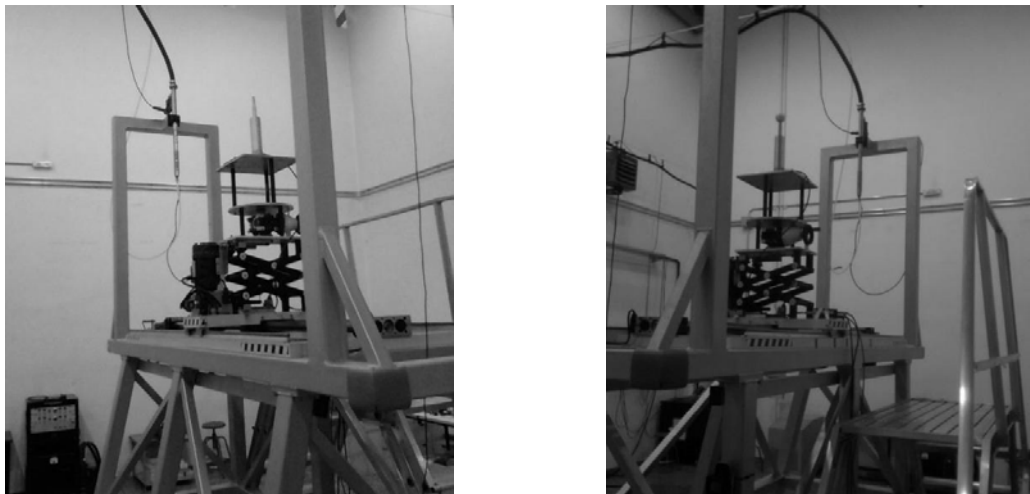


Figure 1. BSS-<sup>6</sup>LiI on the calibration bench (bare detector and 2 inch sphere (BALL 2)).

### 3.- RESULTS

Figure 2 present MCNPX calculated response matrix for all spheres. Figures 3 to 9 show a comparison of the response function for each sphere, calculated in this work, and data published by Vega-Carrillo *et al.*, [2008] and Mares and Schraube [1994a] for the same model of BSS system. Additional data provided by Mares and Schraube [1994b], with the inclusion of more energy bins, are also showed in these graphs.

Figure 10 shows the total neutron lethargy spectrum unfolded from the count rate data obtained with the BSS-<sup>6</sup>LiI system, utilizing the BUNKIUT code for 31 energy bins. Figure 11 shows the total neutron lethargy spectrum unfolded from the same count rate data, utilizing the MAXED computer code from the UMG 3.3 package, with the new calculated response functions, for 222 energy bins.

Figure 12 shows the Total Neutron Lethargy spectrum unfolded from the count rates obtained with the BSS-<sup>3</sup>He system utilizing the MAXED computer code from the UMG 3.3 package, with the specific response functions (CIEMAT-BSS), for 222 energy bins.

Table 1 shows a comparison of the quantities: total fluence and fluence components (thermal, epithermal and fast), ambient dose equivalent ( $H^*(10)$ ) and average energy, for the measurements performed with the BSS-<sup>6</sup>LiI and BSS-<sup>3</sup>He, and unfolded utilizing the BUNKIUT code for 31 energy bins and MAXED for 222 energy bins. For the BUNKIUT code is also showed the error in fitting process. This software does not provide the uncertainties for the quantities mentioned. We have also to emphasize that the  $H^*(10)$  showed in the table for the BUNKIUT code is not that provided by the software. We calculated  $H^*(10)$  folding the neutron energy spectrum (provided by the software) with the fluence-to-ambient dose equivalent conversion coefficients, in  $\text{pSv.cm}^2$ , from the ICRP 74 [ICRP 1996].



For the MAXED code, the uncertainties in the total fluence and  $H^*(10)$  are those provided by the software IQU\_FC33, from the UMG 3.3 package. IQU\_FC33 considers variations in the measured data and in the default spectrum and uses standard methods to do sensitivity analysis and uncertainty propagation [Reginato *et al.* 2004]. Energy ranges considered for the fluence components are: below 0.5 eV for thermal neutrons, between 0.5 eV and 0.1 MeV for epithermal, and above 0.1 MeV for fast neutrons.

Figure 13 shows a comparison of the Total Neutron Lethargy spectra measured with the BSS-<sup>6</sup>LiI and BSS-<sup>3</sup>He and unfolded utilizing the BUNKIUT code for 31 energy bins and MAXED for 222 energy bins.

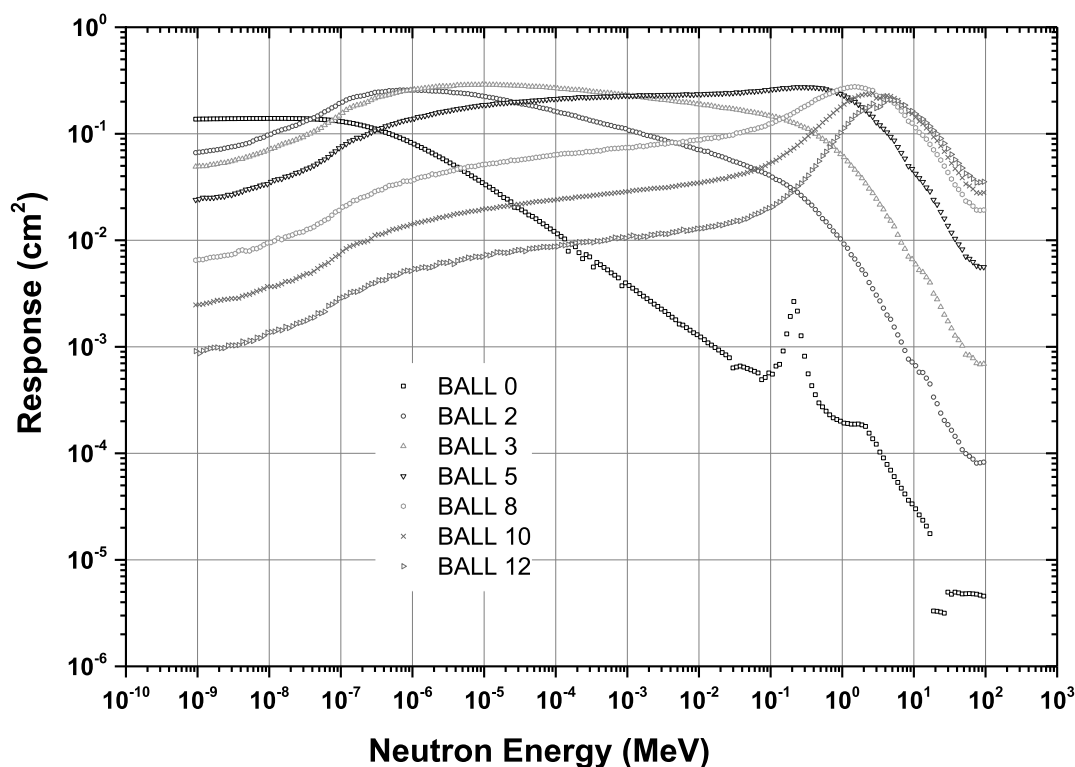


Figure 2. MCNPX calculated response matrix for the BSS-<sup>6</sup>LiI.

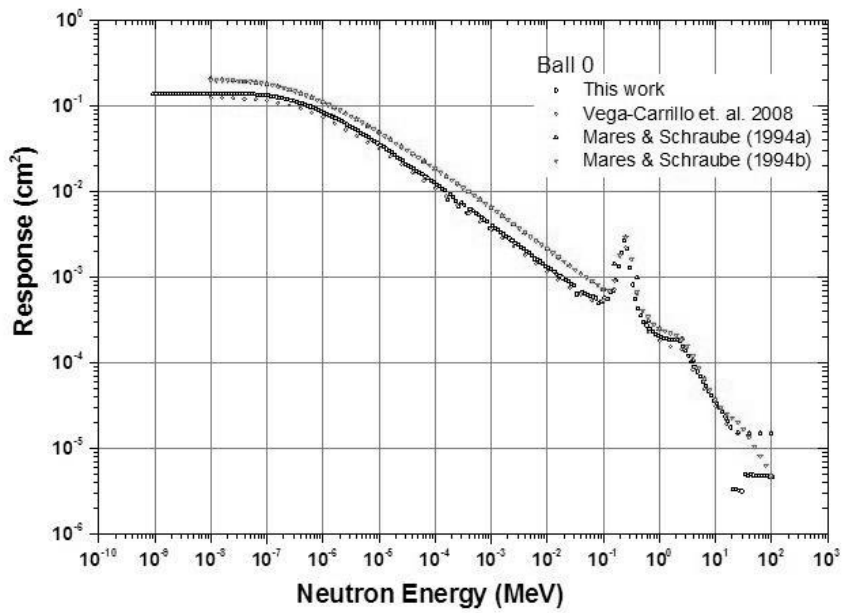


Figure 3. Comparison of the response function for the bare detector (BALL 0), calculated in this work, and other published data.

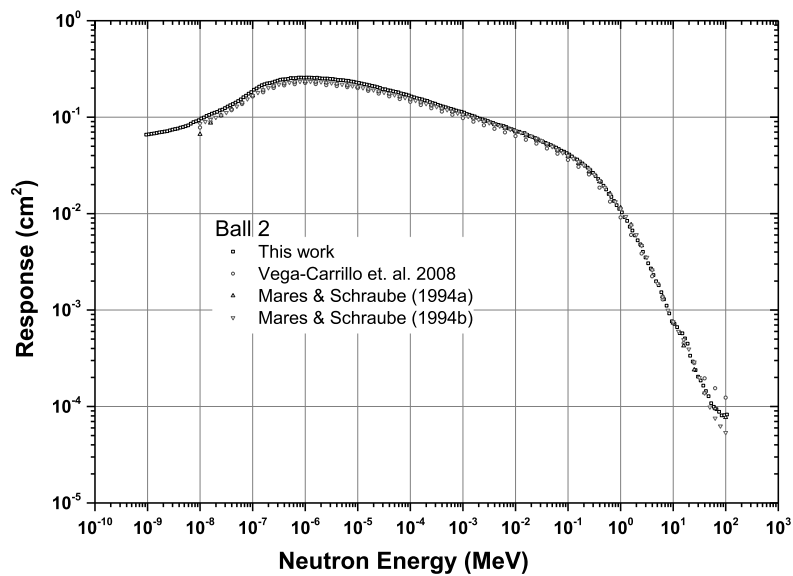


Figure 4. Comparison of the response function for detector with the 2 inch sphere (BALL 2), calculated in this work, and other published data.

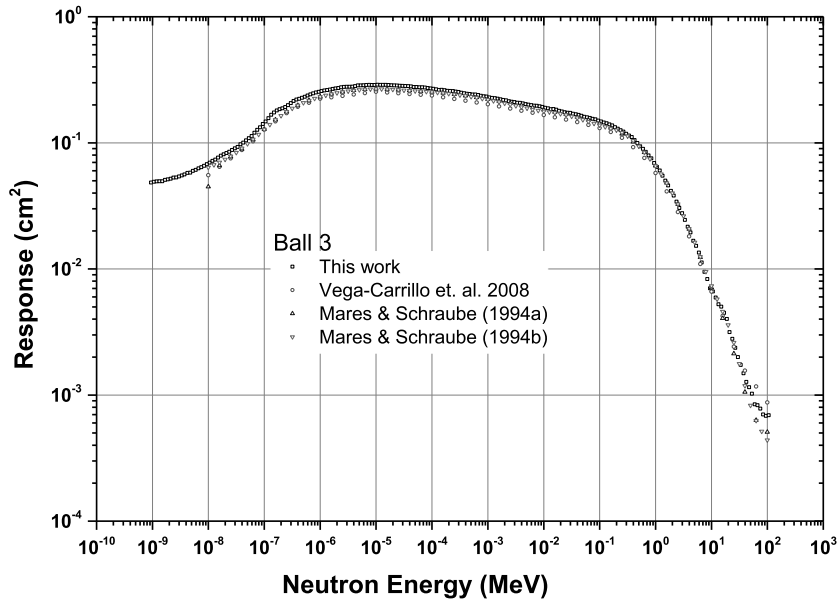


Figure 5. Comparison of the response function for detector with the 3 inch sphere (BALL 3), calculated in this work, and other published data.

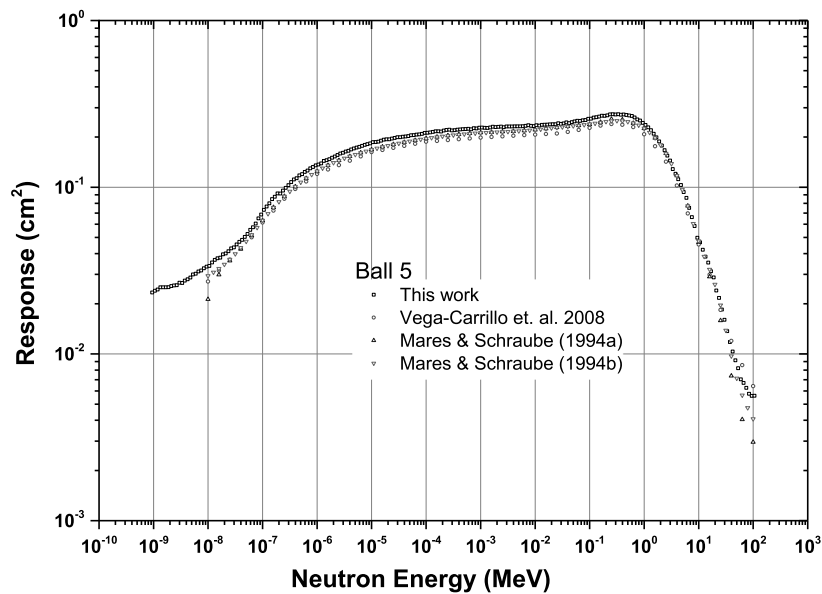


Figure 6. Comparison of the response function for detector with the 5 inch sphere (BALL 5), calculated in this work, and other published data.

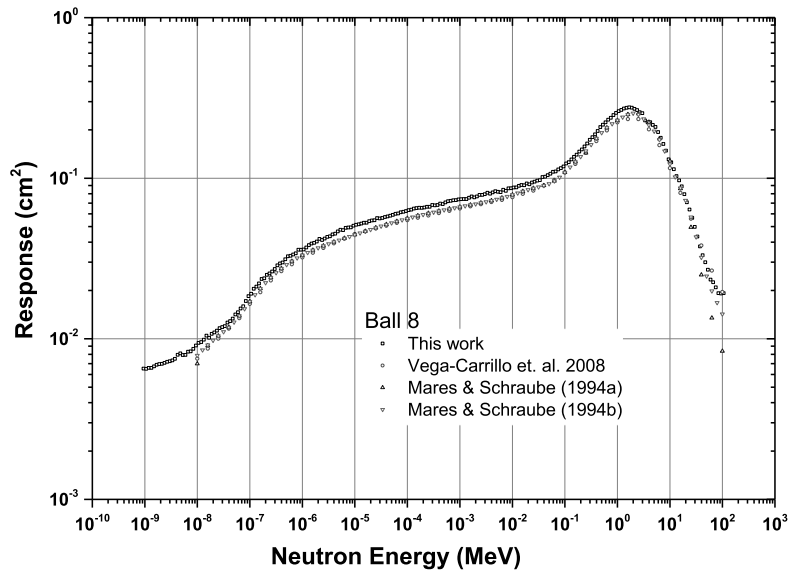


Figure 7. Comparison of the response function for detector with the 8 inch sphere (BALL 8), calculated in this work, and other published data.

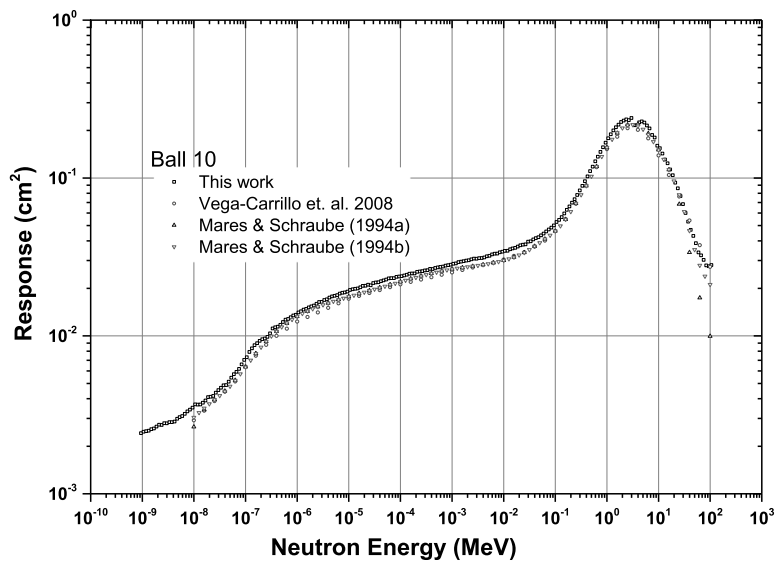


Figure 8. Comparison of the response function for detector with the 10 inch sphere (BALL 10), calculated in this work, and other published data.

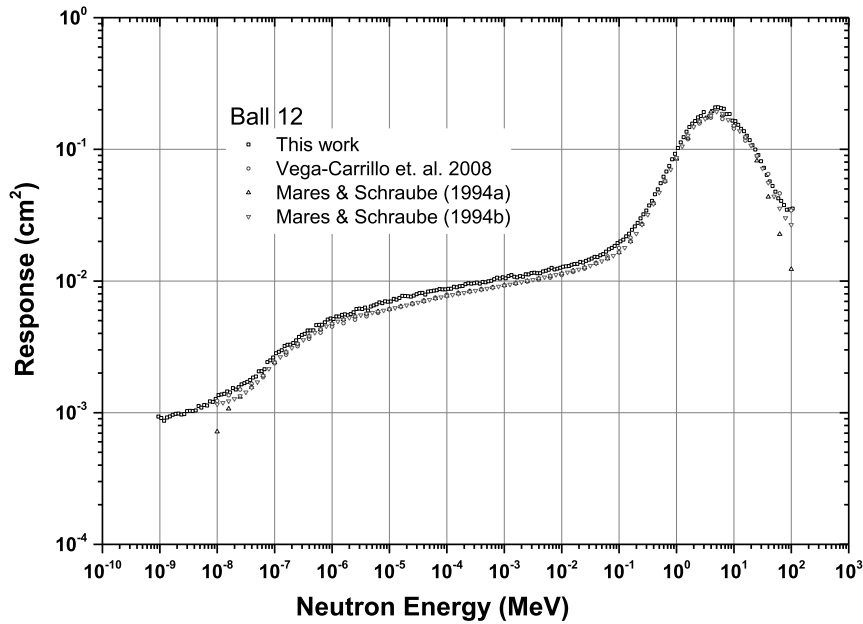


Figure 9. Comparison of the response function for detector with the 12 inch sphere (BALL 12), calculated in this work, and other published data.

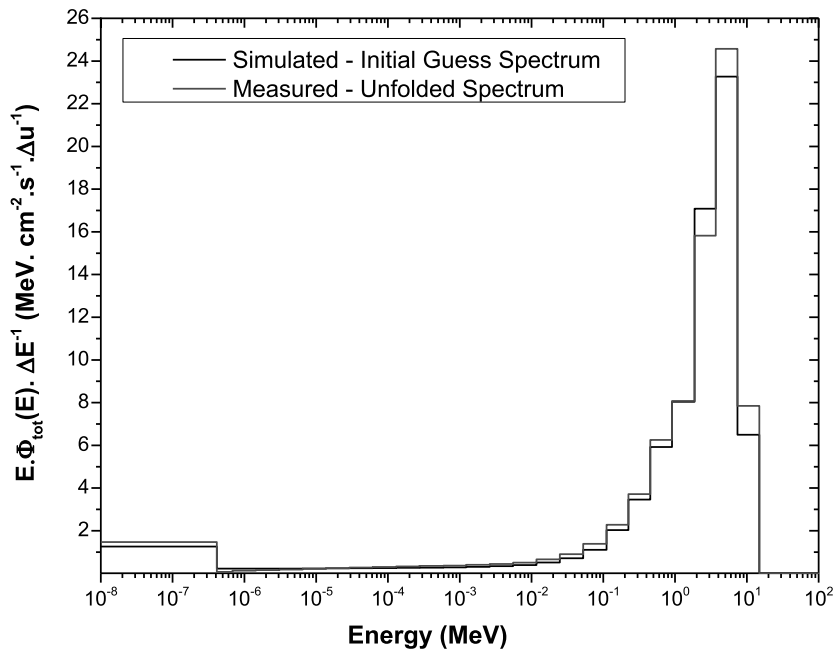


Figure 10. Total Neutron Lethargy Spectrum for the <sup>241</sup>AmBe source of the UPM, at 115 cm, measured with the BSS-<sup>6</sup>LiI system and unfolded with the BUNKIUT code for 31 energy bins.

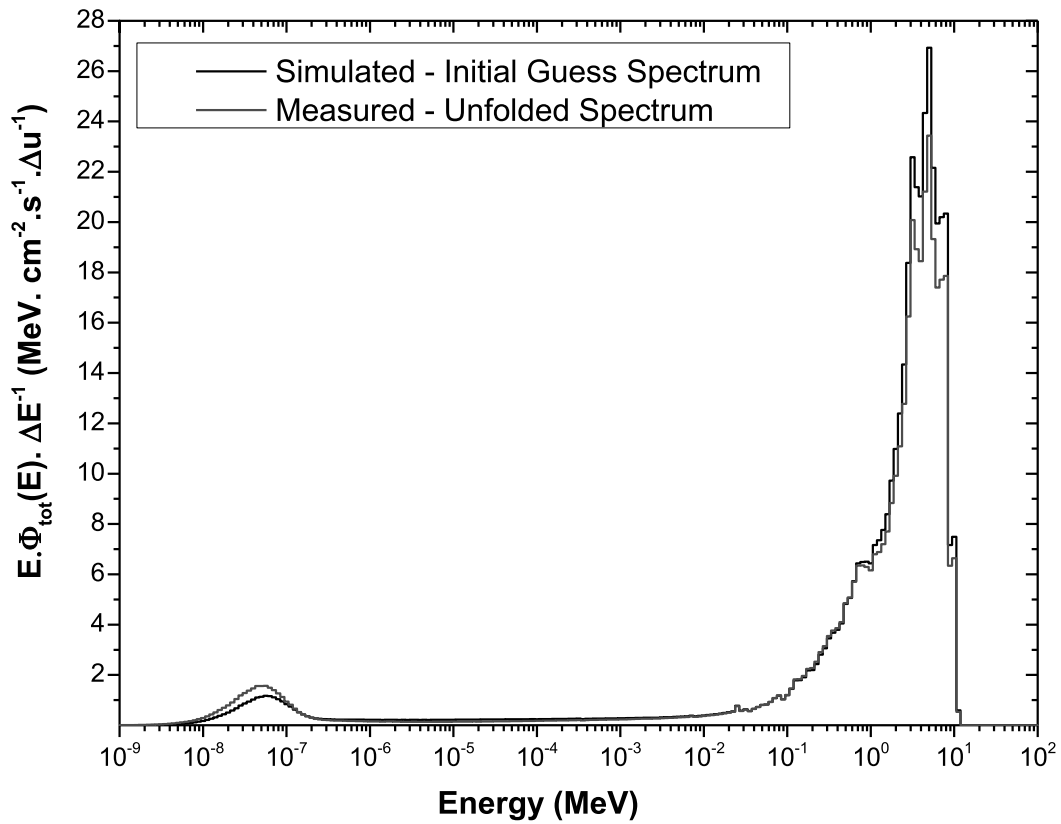


Figure 11. Total Neutron Lethargy Spectrum for the  $^{241}\text{AmBe}$  source of the UPM, at 115 cm, measured with the BSS- $^6\text{LiI}$  system and unfolded with the MAXED computer code from the UMG 3.3 package, with the new calculated response functions (for 222 energy bins).

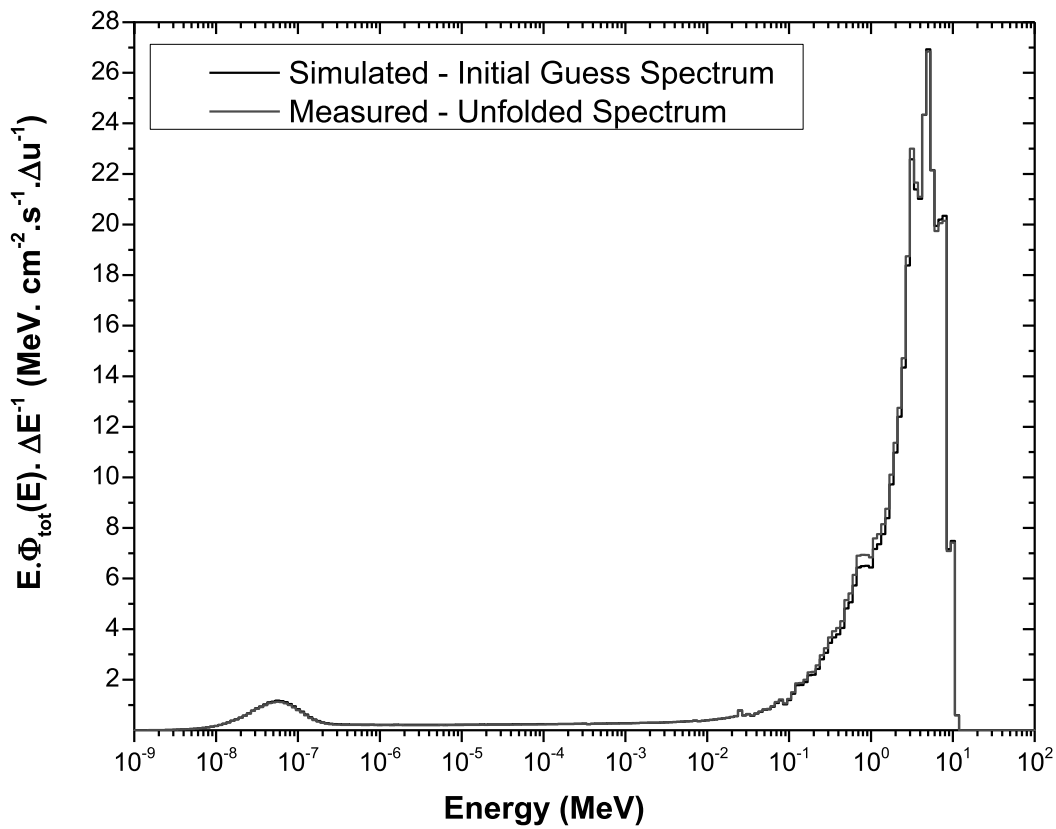


Figure 12. Neutron Lethargy Spectrum for the  $^{241}\text{AmBe}$  source of the UPM, at 115 cm, measured with the BSS- $^3\text{He}$  system and unfolded with the MAXED computer code from the UMG 3.3 package, with the specific response functions (CIEMAT-BSS) for 222 energy bins.

Table 1. Comparison of the quantities: total fluence and fluence components (thermal, epithermal and fast), ambient dose equivalent rate ( $H^*(10)$ ) and average energy for the measurements performed with the BSS-<sup>6</sup>LiI and BSS-<sup>3</sup>He and unfolded utilizing the BUNKIUT code for 31 energy bins and MAXED for 222 energy bins.

	BSS- <sup>6</sup> LiI	BSS- <sup>6</sup> LiI	BSS- <sup>3</sup> He
	BUNKIUT	MAXED	MAXED
<b>Total Fluence rate (<math>\text{cm}^{-2} \cdot \text{s}^{-1}</math>)</b>	53.7	$47.1 \pm 0.43\%$	$51.4 \pm 0.27\%$
$\Phi_{\text{thermal}}$ (%)	5.3	6.7	4.5
$\Phi_{\text{epithermal}}$ (%)	9.2	7.3	7.7
$\Phi_{\text{fast}}$ (%)	85.5	86.0	87.8
<b><math>H^*(10)</math> (<math>\mu\text{Sv/h}</math>)</b>	65.9	$57.4 \pm 0.56\%$	$64.2 \pm 0.31\%$
<b>Average Energy (MeV)</b>	3.6	3.4	3.5
<b>Error of the fit(%)</b>	0.32	-	-

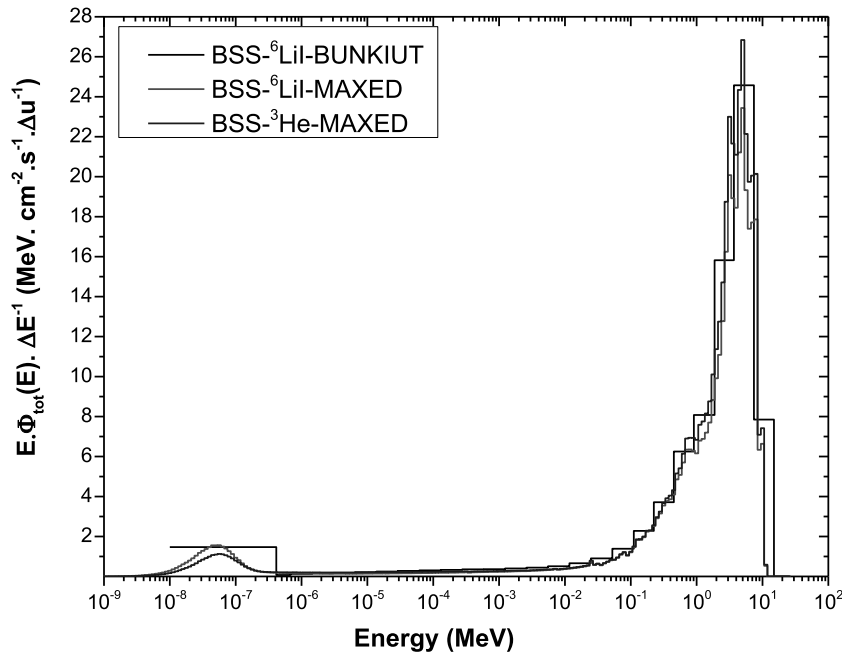


Figure 13. Comparison of the Total Neutron Lethargy spectrum measured with the BSS-<sup>6</sup>LiI and BSS-<sup>3</sup>He and unfolded utilizing the BUNKIUT code for 31 energy bins and UMG for 222 energy bins.



## 4.- DISCUSSION

Figure 2 shows the response functions for all spheres presented an agreement in shape with other available in literature [Mares and Schraube 1994a; Vega-Carrillo *et al.* 2008; Decker *et al.* 2015]. The bare detector (BALL 0) presented a shape close to the shape of the  ${}^6\text{Li}(n,t){}^4\text{He}$  cross section. For the BALL 8 to BALL 12 the responses increase slowly with the neutron energy reaching a maximum value close to 1.7 MeV, 2.4 MeV and 3 MeV, respectively, presenting an accentuated decreasing after that. For the BALL 5 the same behavior is noticed. However, the maximum occurs at about 270 keV. BALL 2 and BALL 3 present an increasing in the responses only up to  $1.1\text{E}(-5)$  and  $1.1\text{E}(-6)$  MeV, respectively. After that, the responses also decrease in a faster manner.

Figures 3 to 9 shows a comparison among between our data and other published elsewhere, for the same detector model. Only BALL 0 did not present a good agreement with Mares and Schraube [1994a,b] for thermal and epithermal energies. This can be attributed not only to the differences in cross-section libraries, but also, to the differences in irradiation setup. Mares and Schraube [1994a,b] calculated the responses for the bare detector, considering a lateral irradiation of the detector, different of the condition simulated in our work.

We can notice a relatively good agreement for BALLS 2 to 12 for energies below 20 MeV. For these spheres, our simulations generally overestimate the responses for energies below 20 MeV. We can also see that there is, in general, an improvement in the agreement as the energy increase. For the BALLS 2 to 12, a higher discrepancy starts to occur for energies close to  $1\text{E}(-8)$  MeV. However, the authors mentioned, did not perform simulations for energies lower than  $1\text{E}(-8)$  MeV. The disagreement can become worst in this energy range and below  $1\text{E}(-8)$ , if an extrapolation of responses behavior is done with the data published by these authors.

For energies above 20 MeV, our data present significant differences with data of Mares and Schraube [1994a,b] for all spheres. Indeed, for the BALL 0, an anomalous behavior is

noticed. We can observe a rapid decreasing followed by an almost constant response. These observations can also be attributed to the differences in cross-section libraries. As the ENDF/B-VII.0 nuclear data library does not have available data for energies higher than 20 MeV, MCNPX utilizes a constant cross section equal to the value at 20 MeV. This adopted value is supposed to be much higher than the real cross section values for energies between 20 MeV and 105.9 MeV. Another point to study is the influence of other nuclear reactions occurring on Lithium ( $^6\text{Li}$  and  $^7\text{Li}$ ) for energies higher than 4 MeV, what we did not take into account in our simulations.

Figure 10 and 11 shows the total neutron lethargy spectra unfolded from the count rate data obtained with a BSS- $^6\text{LiI}$  system, like the modeled in this work. Both spectra exhibited an expected shape for an  $^{241}\text{AmBe}$  source in a vault room with the characteristics of the UPM. Spectrum unfolded with the BUNKIUT code for 31 energy bins exhibited a shape very similar to the initial guess spectrum utilized in the unfolding process and is slightly offset up at all energy range. Already, the spectrum unfolded with the MAXED code and the new response matrix, even exhibiting a shape very similar to the simulated guess spectrum, is offset up in the thermal region and shifted down for energies higher than 2 MeV.

Figure 12 shows the spectrum unfolded from the count rates obtained with the BSS- $^3\text{He}$  system utilizing the MAXED code and CIEMAT-BSS response matrix. In this case, the unfolded spectrum shape very well with the simulated guess spectrum. A comparison of the three spectra is presented in the Figure 13, showing a relatively good agreement at all energy ranges, taking into account the poor energy resolution of the spectrum unfolded with the original BUNKIUT code (with 31 energy bins).

Table 1 shows that spectrum unfolded with MAXED and the new response matrix ( $^6\text{LiI}$ -MAXED) presents a smaller value of total fluence, equivalent dose ( $H^*(10)$ ) and average energy. We can also observe a higher fraction of thermal neutrons ( $\Phi_{\text{thermal}}$ ), respectively 26% and 49% higher than the same fraction observed for BSS- $^6\text{LiI}$ -BUNKIUT and BSS- $^3\text{He}$ -MAXED. The fraction of epithermal neutrons is very close to that observed for BSS- $^3\text{He}$  (within about 5%). Spectrum unfolded with the BUNKIUT code presented a greater

value of  $H^*(10)$ , about 14% higher than the value calculated with the new response matrix and very close ( $< 3\%$ ) to that obtained from BSS- $^3\text{He}$ . Value obtained with the BSS- $^3\text{He}$  was very close to that obtained from MC calculations,  $63.5 \mu\text{Sv/h}$ . On the other hand,  $H^*(10)$  obtained with  $^6\text{Li}$ -MAXED agreed better with measurements performed with a calibrated neutron area monitor BERTHOLD LB6411,  $60.5 \mu\text{Sv/h}$ .

## 5.- CONCLUSIONS

A new response matrix was calculated for a Bonner Sphere Spectrometer (BSS) with a  $^6\text{LiI}(\text{Eu})$  scintillator. Responses were calculated for 6 spheres and the bare detector, for energies varying from  $9.441\text{E}(-10)$  MeV to 105.9 MeV, with 20 equal-log(E)-width bins per energy decade, totalizing 222 energy groups. These response functions were inserted in the response input file of the MAXED code and utilized to unfold the total neutron spectra generated by the  $^{241}\text{AmBe}$  source of the Universidad Politécnica de Madrid (UPM).

A relatively good agreement was observed between our response matrix and that calculated by other authors. In general, we observed an improvement in the agreement as the energy increases. However, higher discrepancies were observed for energies close to  $1\text{E}(-8)$  MeV and, mainly, for energies above 20 MeV. These discrepancies can be mainly attributed to the differences in cross-section libraries employed. However, we need to evaluate the influence of other nuclear reactions occurring on Lithium ( $^6\text{Li}$  and  $^7\text{Li}$ ) for energies higher than 4 MeV, what we did not take into account in our simulations.

Spectrum unfolded with MAXED and the new response matrix ( $^6\text{LiI-MAXED}$ ) presented a smaller value of total fluence, equivalent dose ( $\text{H}^*(10)$ ) and average energy. However, the ambient dose equivalent ( $\text{H}^*(10)$ ) calculated with the  $^6\text{LiI-MAXED}$  showed a good agreement with values measured with the neutron area monitor Berthold LB 6411 and within 12% the value obtained with another BSS system ( $^3\text{He-BSS}$ ).

The response matrix calculated in this work can be utilized together with the MAXED code to generate neutron spectra with a good energy resolution up to 20 MeV. Some additional tests are being done to validate this response matrix and improve the results for energies higher than 20 MeV.

## Acknowledgments

M.A.S. Lacerda is grateful to CNPq (Brazilian National Council for Scientific and Technological Development) for a postdoctoral fellowship (Proc. 233341/2014-5). M.A.S. Lacerda is also grateful to financial support provided by CNPq (MCTI/CNPq/Universal Proc. 449199/2014-2) and FAPEMIG (Research Support Foundation of Minas Gerais State, Brazil) (PPM-00208-15).

## REFERENCES

- Aroua A; Grecscu M; Lanfranchi M; Lerch P; Prête S; Valley JF. (1992). *Evaluation and test of the response matrix of a multisphere neutron spectrometer in a wide energy range. Part II: Simulation*. Nuclear Instruments and Methods **A321**, 305-311.
- Awschalow M; Sanna RS. (1985). *Applications of Bonner detectors in neutron field dosimetry*. Radiation Protection Dosimetry **10**: 89-101.
- Bedogni R; Esposito A; Gentile A; Angelone M; Gualdrini G. (2008). *Determination and validation of a response matrix for a passive Bonner Sphere Spectrometer based on gold foils*. Radiation Measurements **43**:1104-1107.
- Bedogni R; Domingo C; Esposito A; Fernandez F. (2007). *FRUIT: an operational tool for multisphere neutron spectrometry in workplaces*. Nuclear Instruments and Methods in Physics Research A **580**: 1301-1309.
- Bramblett RL; Ewing RI; Bonner TW. (1960). *A new type of neutron spectrometer*. Nuclear Instruments and Methods **9**: 1-12.
- Decker AW; McHale SR; Shannon MP; Clinton JA; McClory JW. (2015). *Novel Bonner Sphere Spectrometer Response Functions Using MCNP6*. IEEE Transactions on Nuclear Science **62(4)**: 1-6.
- Garny S; Mares V; Rühm W. (2009). *Response functions of a Bonner sphere spectrometer calculated with GEANT4*. Nucl. Instrum. Meth. Phys. Research A 604, p.612-617, 2009.
- Hertel, N.E., Davidson, J.W. (1985). *The response of Bonner spheres to neutrons from thermal energies to 17.3 MeV*. Nuclear Instruments and Methods in Physics Research A **238**: 509-516.

- ICRP. (1996). International Commission on Radiological Protection. *Conversion coefficients for use in radiological protection against external radiation*. **ICRP Publication 74**, Ann. ICRP 26 (3-4).
- Los Alamos National Laboratory. (2008). *MCNP-A General Monte Carlo N-Particle Transport Code, version 5*. X-5 Monte Carlo Team. **LA-UR-03-1987**.
- Lowry KA; Johnson TL. (1984). *Modifications to recursion unfolding algorithms to and more appropriate neutron spectra*. Health Physics **47**: 587-593.
- Mares V; Schraube G; Schraube H. (1991). *Calculated neutron response of a Bonner Sphere Spectrometer with <sup>3</sup>He counter*. Nuclear Instruments and Methods in Physics Research A **307**: 398-412.
- Mares V; Schraube H. (1994a). *Evaluation of the Response Matrix of a Bonner Sphere Spectrometer with LiI detector from thermal energy to 100 MeV*. Nuclear Instruments and Methods in Physics Research A **337**: 461-473.
- Mares V; Schraube H. (1994b). Personal communication.
- Martinez-Blanco MR; Ortiz-Rodriguez JM; Vega-Carrillo HR. (2009). *NSDann, a LabVIEW tool for neutron spectrometry and dosimetry based on the RDANN methodology*. Proceedings of the Electronics, Robotics and Automotive Mechanics Conference, CERMA'09 131-136.
- Matzke M. (2002). *Propagation of uncertainties in unfolding procedures*. Nuclear Instruments and Methods in Physics Research A **476**: 230-241.
- Mazrou H; Idiri Z; Sidahmed T; Allab M. (2010). *MCNP5 evaluation of a response matrix of a Bonner Sphere Spectrometer with a high efficiency <sup>6</sup>LiI(Eu) detector from 0.01 eV to 20 MeV neutrons*. Journal of Radioanalytical and Nuclear Chemistry **284**: 253-263.
- McDonald JC; Siebert BRL; Alberts WG. (2002). *Neutron spectrometry for radiation protection purposes*. Nuclear Instruments and Methods in Physics Research A **476**: 347-352.
- Pelowitz DB. (2011). *MCNPX User's Manual, Version 2.7.0*. Los Alamos National Laboratory **Report LA-CP-11-00438**.
- Reginatto M; Wiegel B; Zimbal A; Langner F. (2004). *The 'few-channel' unfolding programs in the UMG package: MXD\_FC31 and IQU\_FC31, and GRV\_FC31, version 3.1*, Physikalisch-Technische Bundesanstalt (PTB).

- Reginatto M; Goldhagen P; Neumann S. (2002). *Spectrum unfolding, sensitivity analysis and propagation of uncertainties with the maximum entropy deconvolution code MAXED*. Nuclear Instruments and Methods in Physics Research A **476**: 242-246.
- Sanna RS. (1973). *Thirty-One Group Response Matrices for the Multisphere Neutron Spectrometer over the energy range thermal to 400 MeV*. USAEC, **Report HASL-267**.
- Sannikov AV. (1994). *BON94 code for neutron spectra unfolding from Bonner spectrometer data*. CERN internal Report **CERN/TIS-RP/IR/94-16**.
- Seltzer, SM; Berger MJ. (1982). *Evaluation of the collision stopping power of elements and compounds for electrons and positrons*. The International Journal of Applied Radiation and Isotopes 33: 1189-1218.
- Thomas DJ; Alevra AV. (2002). *Bonner sphere spectrometers – a critical review*. Nuclear Instruments and Methods in Physics Research A **476**: 12-20.
- Vega-Carrillo HR; Wehring BW; Veinot KG; Hertel NE. (1999). *Response matrix for a multisphere spectrometer using <sup>6</sup>LiF thermoluminescence dosimeter*. Radiation Protection Dosimetry **81**: 133-140.
- Vega-Carrillo HR; Donaire I; Gallego E; Manzanares-Acuña E; Lorente A; Iñiguez MP; Martin-Martin A; Gutierrez-Villanueva JL. (2008). *Calculation of Response matrix of a BSS with <sup>6</sup>LiI scintillator*. Revista Mexicana de Física **54**: 57-62.
- Vega-Carrillo HR; Gallego E; Lorente, A; Rubio IP; Méndez R. (2012). *Neutron features at the UPM neutronics hall*. Applied Radiation and Isotopes **70**: 1603-1607.
- Wiegel B; Alevra AV. (2002). *NEMUS-The PTB Neutron Multisphere Spectrometer: Bonner spheres and more*. Nuclear Instruments and Methods in Physics Research A **476**: 36-41.